

# Search for TeV Emission from the Direction of the Vela and PSR B1706–44 Pulsars with the H.E.S.S. Experiment

B. Khélifi\*, Nu. Komin†, T. Lohse†, C. Masterson\*, S. Schlenker†,  
F. Schmidt†, U. Schwanke† and C. Stegmann†  
for the H.E.S.S. collaboration

\**Max-Planck-Institut für Kernphysik, P.O. Box 103980, D-69029 Heidelberg, Germany*

†*Institut für Physik, Humboldt-Universität zu Berlin, Newtonstr. 15, D-12489 Berlin, Germany*

**Abstract.** The pulsar wind nebulae (PWN) around the Vela and PSR B1706–44 pulsars have been observed in 2003 and 2004 with the H.E.S.S. Cherenkov telescopes. No evidence of a  $\gamma$ -ray emission from either source is seen and upper limits on the integrated flux are reported.

## INTRODUCTION

Massive stars (greater than 10 solar masses) can end their lives in supernova explosions and may collapse into neutron stars, creating so-called filled-centre or *plerionic* supernova remnants. These neutron stars have the potential to produce very high energy (VHE)  $\gamma$ -rays.

Neutron stars have a surface magnetic field of the order of  $10^{12}$  G and an initial rotational period between 10 and 100 ms. The total energy available for the pulsar to power the plerion is of the order  $10^{49}$  erg. A significant fraction of the rotational energy of the pulsar is thought to be carried away by a relativistic wind of electrons and positrons (with a possible hadronic component). The interaction of this wind with the surrounding medium creates a relativistic shock, where the leptons can be accelerated to high energies [1, 2]. Alternatively, the lepton acceleration could be driven by the reconnection of the alternating magnetic field at the pulsar wind termination shock [3]. The interaction of accelerated leptons with ambient photon fields (e.g. the cosmic microwave background, local infrared photons) can produce VHE  $\gamma$ -rays via the Inverse Compton process.

The first established emitter of VHE  $\gamma$ -rays, the Crab nebula, is a plerionic supernova remnant. The observation of further objects of this type allows to test the current understanding of their evolution and particle acceleration mechanisms.

## OBSERVATIONS WITH H.E.S.S.

The H.E.S.S. experiment [4] is an imaging atmospheric Cherenkov detector dedicated to the observation of VHE  $\gamma$ -rays. Situated in Namibia, the full 4-telescope array is operational since December 2003. Each telescope has a mirror area of 107 m<sup>2</sup> and is equipped with a camera consisting of 960 photomultiplier tubes [5]. The system has a field of view of 5° and allows to reconstruct the direction of individual showers with a precision better than 0.1° ([6], [7], [8]).

The spatial resolution achieved with H.E.S.S. implies that the Vela and PSR B1706–44 pulsars and pulsar wind nebulae appear as point-like objects. The two pulsars were observed with H.E.S.S. between April and July 2003 (PSR B1706–44) and between January and March 2004 (Vela).

## DATA ANALYSIS TECHNIQUE

The recorded data were subjected to numerous checks concerning hardware stability and weather conditions. Only high-quality data were considered for analysis. After calibration and image cleaning, showers were reconstructed using standard techniques ([9], [10]). Cuts on scaled Hillas parameters as described in [11] were applied in order to reduce the hadronic background. These cuts were optimised for weak signals of about 10 % of the Crab flux. Gamma-like events are searched for by comparing events coming from the assumed source position (ON region) with events from control regions in the same field of view (OFF regions). An excess of signal events can be found in the distribution of  $\Theta^2$ , where  $\Theta$  is the angle between the reconstructed shower direction and the direction of the investigated source.

Limits on the integrated flux above certain energies  $E_T$  were obtained using two different methods. The first (model-dependent) method counts events with energies above  $E_T$  and compares with the expected number assuming a power law for the differential flux

$$\frac{d\Phi}{dE} \propto \left( \frac{E}{E_0} \right)^{-\Gamma}$$

with a photon index  $\Gamma$ . The second (model-independent) method avoids the assumption of a power law and calculates the integrated flux  $F$  directly as the difference of the fluxes from the ON and OFF regions

$$F(> E_T) = \frac{1}{T} \left( \sum_{i=1}^{N_{\text{on}}} \frac{1}{A_i} - \delta \sum_{i=1}^{N_{\text{off}}} \frac{1}{A_i} \right).$$

Here,  $T$  is the live time, and the first (second) sum runs over all showers with reconstructed energies greater than  $E_T$  in the ON (OFF) region. The  $A_i$  are the effective areas which depend on the zenith angle and energy of each event, and  $\delta$  is a factor accounting for differences in size and acceptance between the ON and OFF regions.

**TABLE 1.** Observation details of the discussed data sets. The energy thresholds for the corresponding mean zenith angle has been estimated from Monte Carlo simulations.

	number of telescopes	mean zenith angle	energy threshold	live time
Vela, data set 1	3	30°	250 GeV	6.2 h
Vela, data set 2	4	35°	280 GeV	5.2 h
PSR B1706–44	2	27°	310 GeV	14.3 h

**TABLE 2.** Upper limits with 99.9% confidence level (CL) on the integrated flux from the Vela pulsar direction in units of  $\text{s}^{-1}\text{cm}^{-2}$ .

	photon index 2.5		model-independent	
	pulsar position	CANGAROO pos.	pulsar position	CANGAROO pos.
F(E>500 GeV)	$1.2 \cdot 10^{-12}$	$3.3 \cdot 10^{-12}$	$1.2 \cdot 10^{-12}$	$3.3 \cdot 10^{-12}$
F(E>1 TeV)	$7.4 \cdot 10^{-13}$	$1.8 \cdot 10^{-12}$	$8.2 \cdot 10^{-13}$	$2.0 \cdot 10^{-12}$
F(E>2.5 TeV)	$2.7 \cdot 10^{-13}$	$7.6 \cdot 10^{-13}$	$3.1 \cdot 10^{-13}$	$9.5 \cdot 10^{-13}$

## RESULTS FOR THE VELA PULSAR (PSR B0833–45)

The Vela pulsar at a distance of around 300 pc is one of the brightest pulsars in soft  $\gamma$ -rays as seen by EGRET [12]. The pulsar wind nebula has been detected in X-rays by CHANDRA [13]. CANGAROO reported a detection in VHE  $\gamma$ -rays at a position  $0.13^\circ$  south-east of the pulsar with an integrated flux above 2.5 TeV of  $(2.9 \pm 0.5 \pm 0.4) \cdot 10^{-12} \text{s}^{-1}\text{cm}^{-2}$  and a photon index of 2.5 [14]. This detection could not be verified in a later work and an upper limit on the integrated flux above 2.7 TeV of  $2.5 \cdot 10^{-12} \text{s}^{-1}\text{cm}^{-2}$  has been calculated [15].

The Vela data were recorded with the complete H.E.S.S. array of four telescopes and an array-level hardware trigger [16] for a total live time of 11.4 h. The data comprise two different detector configurations with three telescopes (data set 1) and four telescopes (data set 2). The corresponding zenith angles, energy thresholds and live times are shown in Table 1. The analysis has been made for the pulsar position at (RA 8h35m20.66s, Dec  $-45^\circ 10' 35.2''$ ) and for the position  $0.13^\circ$  to the south-east (RA 8h34m57.6s, Dec  $-45^\circ 16' 48''$ ) (CANGAROO position). A  $\Theta^2$  cut of 0.02 degrees<sup>2</sup> has been applied to the data at the pulsar position. In order to reproduce the larger point spread function of the CANGAROO experiment (HWHM  $\sim 0.18^\circ$  [14]), the  $\Theta^2$  cut was relaxed to 0.05 degrees<sup>2</sup> for the CANGAROO position.

No excess is observed in any of the two data sets at both test positions (Figure 1). Upper limits (99.9% confidence level (CL), Helene method [17]) on the integrated flux have been calculated using the model-independent and model-dependent method (with an assumed photon index of 2.5). The results are summarised in Table 2.

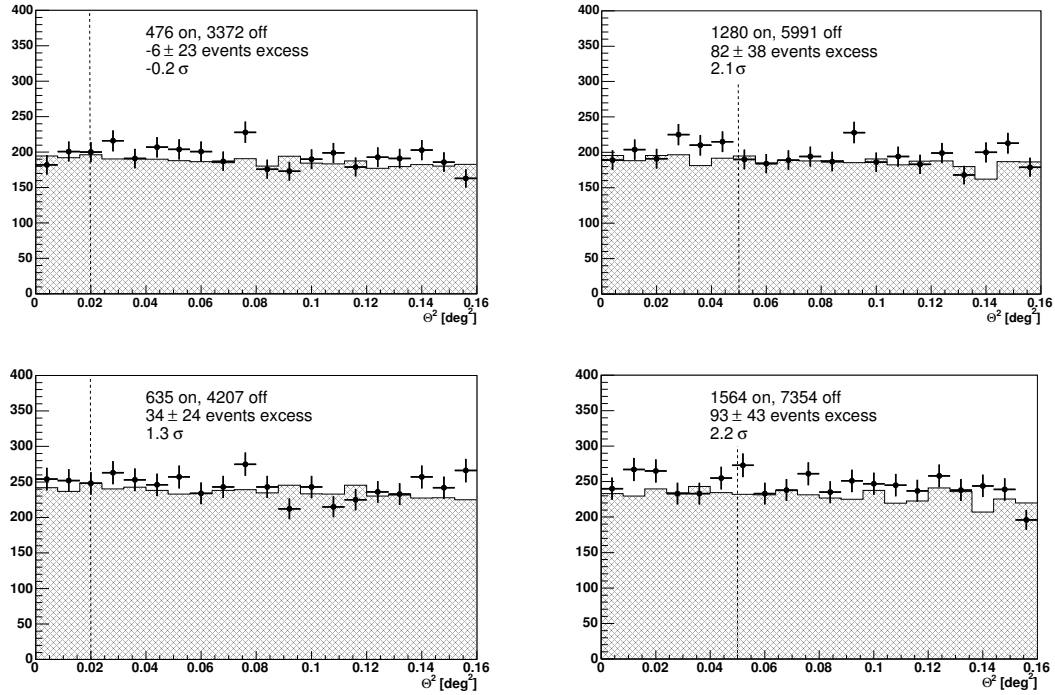


**FIGURE 1.**  $\Theta^2$  distributions for the Vela data set 1 (top row) and data set 2 (bottom row). The left column shows the plots for the Vela pulsar position, the right column for the CANGAROO position. The points denote events from the source region. The shaded histograms show events from background regions. They were scaled to the statistics of the source region. The dashed lines denote the applied  $\Theta^2$  cuts of 0.02 degrees<sup>2</sup> for the pulsar position and 0.05 degrees<sup>2</sup> for the CANGAROO position.

## RESULTS FOR PSR B1706–44

For PSR B1706–44, pulsed emission has been found in radio, X-rays and soft  $\gamma$ -rays. Around the pulsar, an extended synchrotron nebula has been observed in radio and also in X-rays, suggesting the existence of a pulsar wind nebula powered by the pulsar. In the TeV range, the experiments CANGAROO and Durham Mark 6 detected a steady emission of  $8 \cdot 10^{-12} \text{s}^{-1} \text{cm}^{-2}$  above 1 TeV [18] and  $(3.9 \pm 0.7_{stat}) \cdot 10^{-11} \text{s}^{-1} \text{cm}^{-2}$  above 300 GeV [19], respectively, coincident with the PWN position.

PSR B1706–44 was observed with two telescopes in the commissioning phase of the H.E.S.S. experiment for a total live time of 14.3 h. The energy threshold and mean zenith angle of the observations are shown in Table 1. Since data had been recorded without a central trigger, events were combined in software using their GPS time stamps. The resulting  $\Theta^2$  plot for the pulsar position is shown in Figure 2. No significant excess is observed. Helene upper limits (99.9% CL) on integrated fluxes above 500 GeV and 1 TeV were calculated employing both the model-independent and the model-dependent method. For the latter, the photon index of 2.5 reported by the CANGAROO experiment was used. Both methods give very similar results which are summarised in Table 3.

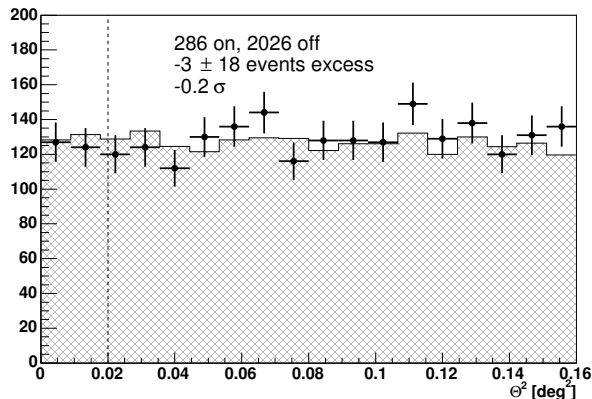


**FIGURE 2.**  $\Theta^2$  distribution from observations of PSR B1706–44. The points denote events from the source region, the shaded histogram is the background. The background is scaled to the statistics of the source region. The dashed line denotes the applied  $\Theta^2$  cut of 0.02 degrees<sup>2</sup>.

**TABLE 3.** Upper limits (99.9% CL) on the integrated flux from PSR B1706–44 in units of  $\text{s}^{-1}\text{cm}^{-2}$ .

	photon index 2.5	model-independent
F(E>500 GeV)	$1.1 \cdot 10^{-12}$	$9.7 \cdot 10^{-13}$
F(E>1 TeV)	$4.2 \cdot 10^{-13}$	$3.8 \cdot 10^{-13}$

## SUMMARY

The H.E.S.S. experiment detected no significant VHE  $\gamma$ -ray signals from the direction of the Vela and PSR B1706–44 pulsars. For Vela, we set an upper limit on the integrated flux above 2.5 TeV of  $7.6 \cdot 10^{-13} \text{s}^{-1}\text{cm}^{-2}$  assuming a photon index of 2.5. This limit is at a level of 26 % of the flux measured by CANGAROO [14] but it is consistent with the CANGAROO upper limit shown in [15].

For PSR B1706–44, the upper limit on the integrated flux above 1 TeV is  $4.2 \cdot 10^{-13} \text{s}^{-1}\text{cm}^{-2}$  assuming the photon index of 2.5 from an earlier CANGAROO detection. This limit corresponds to 5 % of the reported CANGAROO flux.

These results are preliminary and the evaluation of systematic errors is pending.

## ACKNOWLEDGMENTS

The support of the Namibian authorities and of the University of Namibia in facilitating the construction and operation of H.E.S.S. is gratefully acknowledged, as is the support by the German Ministry for Education and Research (BMBF), the Max Planck Society, the French Ministry for Research, the CNRS-IN2P3 and the Astroparticle Interdisciplinary Programme of the CNRS, the U.K. Particle Physics and Astronomy Research Council (PPARC), the IPNP of the Charles University, the South African Department

of Science and Technology and National Research Foundation, and by the University of Namibia. We appreciate the excellent work of the technical support staff in Berlin, Durham, Hamburg, Heidelberg, Palaiseau, Paris, Saclay, and in Namibia in the construction and operation of the equipment.

## REFERENCES

1. Gallant, Y. A., “Particle Acceleration at Relativistic Shocks,” in *Lecture Notes in Physics, Berlin Springer Verlag*, 2002, vol. 589, pp. 24–+.
2. Aharonian, F. A., Atoyan, A. M., and Kifune, T., *MNRAS*, **291**, 162–176 (1997).
3. Komissarov, S. S., and Lyubarsky, Y. E., *MNRAS*, **344**, L93–L96 (2003).
4. Hofmann, W., “Status of the H.E.S.S. Project,” in *Proc. 28th ICRC, Tsukuba*, Univ. Academy Press, Tokyo, p. 2811.
5. Vincent, P., Denance, J.-P., and Huppert, J.-F. et al., “Performance of the H.E.S.S. cameras,” in *Proc. 28th ICRC, Tsukuba*, Univ. Academy Press, Tokyo, p. 2887.
6. Gillessen, S., for the H.E.S.S. collaboration, “Arcsecond Level Pointing Of The H.E.S.S. Telescopes,” in *Proc. 28th ICRC, Tsukuba*, Univ. Academy Press, Tokyo, p. 2899.
7. Aharonian, F. et al. (H.E.S.S. collaboration), *Astroparticle Physics*.
8. Bernlöhner, K., Carrol, O., Cornils, R., Elfahem, S., Espigat, P., Gillessen, S., Heinzlmann, G., Hermann, G., Hofmann, W., Horns, D., Jung, I., Kankanyan, R., Katona, A., Khelifi, B., Krawczynski, H., Panter, M., Punch, M., Rayner, S., Rowell, G., Tluczykont, M., and van Staa, R., *Astroparticle Physics*, **20**, 111–128 (2003).
9. Hillas, A. M., “Cerenkov light images of EAS produced by primary gamma,” in *NASA. Goddard Space Flight Center 19th Intern. Cosmic Ray Conf., Vol. 3 p 445-448 (SEE N85-34862 23-93)*, 1985, vol. 3, pp. 445–448.
10. Aharonian, F. A. et al. (HEGRA collaboration), *A&A*, **349**, 11–28 (1999).
11. Aharonian, F. A. et al. (H.E.S.S. collaboration), “H.E.S.S. observations of PKS 2155–304”, *accepted for publication in A&A* (2004).
12. Fierro, J. M., Michelson, P. F., Nolan, P. L., and Thompson, D. J., *ApJ*, **494**, 734+ (1998).
13. Pavlov, G. G., Teter, M. A., Kargaltsev, O., and Sanwal, D., *ApJ*, **591**, 1157–1171 (2003).
14. Yoshikoshi, T., Kifune, T., Dazeley, S. A., Edwards, P. G., Hara, T., Hayami, Y., Kakimoto, F., Konishi, T., Masaike, A., Matsubara, Y., Matsuoka, T., Mizumoto, Y., Mori, M., Muraishi, H., Muraki, Y., Naito, T., Nishijima, K., Oda, S., Ogio, S., Ohsaki, T., Patterson, J. R., Roberts, M. D., Rowell, G. P., Sako, T., Sakurazawa, K., Susukita, R., Suzuki, A., Tamura, T., Tanimori, T., Thornton, G. J., Yanagita, S., and Yoshida, T., *ApJ*, **487**, L65+ (1997).
15. Dazeley, S. A., Patterson, J. R., Rowell, G. P., and Edwards, P. G., *Astroparticle Physics*, **15**, 313–321 (2001).
16. Funk, S. et al., *accepted for publication in Astropart. Phys., “The trigger system of the H.E.S.S. telescope array”* (2004).
17. Helene, O., *NIM*, **212**, 319 (1983).
18. Kifune, T., Tanimori, T., Ogio, S., Tamura, T., Fujii, H., Fujimoto, M., Hara, T., Hayashida, N., Kabe, S., Kakimoto, F., Matsubara, Y., Mizumoto, Y., Muraki, Y., Suda, T., Teshima, M., Tsukagoshi, T., Watase, Y., Yoshikoshi, T., Edwards, P. G., Patterson, J. R., Roberts, M. D., Rowell, G. P., and Thornton, G. J., *ApJL*, **438**, L91–L94 (1995).
19. Chadwick, P. M., Dickinson, M. R., Dipper, N. A., Holder, J., Kendall, T. R., McComb, T. J. L., Orford, K. J., Osborne, J. L., Rayner, S. M., Roberts, I. D., Shaw, S. E., and Turver, K. E., *Astroparticle Physics*, **9**, 131–136 (1998).